Dynamics of the in-run in ski jumping: a simulation study

Ettema, G.J.; Braten, S.; Bobbert, M.F.

published in
Journal of Applied Biomechanics
2005

DOI (link to publisher)
10.1123/jab.21.3.247

document version
Publisher's PDF, also known as Version of record

JOURNAL OF APPLIED BIOMECHANICS, 2005, **21**, 247-259

Dynamics of the In-Run in Ski Jumping: A Simulation Study

Gertjan J.C. Ettema[1], Steinar Bråten[1], and Maarten F. Bobbert[2]
[1]Norwegian University of Science and Technology
[2]Vrije Universiteit Amsterdam

A ski jumper tries to maintain an aerodynamic position in the in-run during changing environmental forces. The purpose of this study was to analyze the mechanical demands on a ski jumper taking the in-run in a static position. We simulated the in-run in ski jumping with a 4-segment forward dynamic model (foot, leg, thigh, and upper body). The curved path of the in-run was used as kinematic constraint, and drag, lift, and snow friction were incorporated. Drag and snow friction created a forward rotating moment that had to be counteracted by a plantar flexion moment and caused the line of action of the normal force to pass anteriorly to the center of mass continuously. The normal force increased from 0.88G on the first straight to 1.65G in the curve. The required knee joint moment increased more because of an altered center of pressure. During the transition from the straight to the curve there was a rapid forward shift of the center of pressure under the foot, reflecting a short but high angular acceleration. Because unrealistically high rates of change of moment are required, an athlete cannot do this without changing body configuration which reduces the required rate of moment changes.

Key Words: musculoskeletal system, muscular coordination, sport

Ski jumping is a sport that makes extreme demands on the athletes. Many studies have been conducted of the take-off and flight in ski jumping. A main issue has been, and still is, how to optimize the athlete's movements for maximal performance. Most researchers agree that the push-off action, take-off, and early flight phase (transition from take-off to flight) are crucial (e.g., Virmavirta, Kikeväs, & Komi, 2001a; Virmavirta, Perttunen, & Komi, 2001b). However, the in-run, which consists of a curved path in between two straights, is also considered to be important because what the athlete does during the in-run determines the initial conditions for take-off.

[1]Human Movement Sciences Program, Faculty of Social Sciences and Technology Management, Norwegian University of Science and Technology (NTNU), 7491 Trondheim, Norway; [2]Institute for Fundamental and Clinical Human Movement Science, Vrije Universiteit Amsterdam, Van der Boechorststraat 9, 1081 BT Amsterdam, The Netherlands.

To date, little attention has been paid to the dynamics of the in-run. At first glance the demands on the athlete seem relatively straightforward: maintain an aerodynamic squat position by withstanding the increasing (centripetal) ground forces during the curved part of the hill. However, when gliding through the curved part, the athlete not only experiences increasing ground forces but also undergoes (backward) rotation, i.e., acquires an angular momentum. This occurs under circumstances when the drag force and the force of friction between skis and hill create progressively increasing external moments. Because both forces have their center of application below the center of mass (Ettema & Bråten, 2004), they tend to cause forward angular acceleration of the athlete. There seem to be two extra demanding sections of the in-run, the curve entrance and the curve exit. In the curve entrance section, the change of path from straight to curve introduces a sudden demand for rotation. The curve exit section makes the opposite demand in that the rotation must suddenly be stopped. The curve exit is especially important as it is also (near) the point of onset of the push-off action.

To gain more insight into ski jumping, various studies have been performed. However, because of the practical difficulties with data collection, the experimental data available on the in-run (including take-off table) is incomplete. Information on various important variables such as frictional forces and point of application (center of pressure) of ground reaction forces is missing (Tveit & Pedersen, 1981; Virmavirta & Komi, 1989, 1993; see also Komi & Virmavirta, 2000). Moreover, in experimental studies one does not have full control over the jumper's (re)actions and it is difficult to disentangle the effects of external forces on the one hand and the actions of the athlete (who tries to counteract the undesired effects of the external forces) on the other hand. We therefore analyzed the dynamics of the in-run using computer simulation with a model that had been applied successfully to vertical jumping, cycling, and speed skating (e.g., Bobbert, Houdijk, de Koning, & de Groot, 2002; Pandy, Zajac, Sim, & Levine, 1990; van Soest, Schwab, Bobbert, & van Ingen Schenau, 1993). The simulations are by no means meant to replace experimental studies but merely to provide a useful supplement in the search for key elements in ski jumping.

The question of whether an athlete is able to take the in-run in a stable configuration (at least reasonably well) is already answered in the positive by the reality of practice. The question of what this requires from the athlete, however, is still open. The aim of the present study was to analyze the mechanical demands posed on an athlete, both in terms of external forces that occur and in terms of joint moments that need to be generated when performing this task. For this purpose we considered a rigid dummy sliding down the hill and calculated the joint moments required for the task. For generalization purposes we created simulations under different hill characteristics and different magnitudes of drag and surface friction.

Methods

We simulated the events of a rigid dummy going down the hill and through the in-run (rigid-dummy model). In this model the joint angles were forcefully kept constant and the corresponding joint moment histories were calculated; these joint moment histories would have to be generated by an athlete if he or she were to maintain the static position throughout the in-run.

A forward dynamic model of a ski jumper was obtained by adapting a

model previously described for vertical jumping (van Soest et al., 1993). The model contained four rigid segments foot+boot+ski, leg, thigh, and upper body (trunk, head+helmet, and upper extremities kept to the side of the trunk). Segment parameters were obtained for an average ski jumper (mass 60 kg, height 1.75 m). The ratios of masses, lengths, and moments of inertia of the segments were found by adjusting data from van Soest et al. (1993) for masses of skis, boots, and helmet. The foot was modeled slightly longer than the anatomical length to include the effects of wearing boots and skis. However, the heel was not fixed to the ski, so that plantar flexion was possible and ground reaction forces could not pass anteriorly to the boot+binding support area. The squat position adopted in the in-run was obtained by analysis of various laboratory simulation jumps and was comparable with data from the literature (Komi & Virmavirta, 2000). The initial joint angles were: ankle 50°, knee 77°, and hip 32° (see Figure 1). The model consisted of equations of motion for each segment and equations defining the constraints of the hill, which were integrated over time using the ode45 integrator in Matlab (Mathworks).

The external constraints that were implemented were based on the Granåsen K120 Hill, Trondheim, Norway (Figure 1): a straight of 95-m angle of 146° with horizontal, a curvature with radius of 105 m, and a 6.65-m take-off table with a 169° angle. Additional comparisons were made with the K90 Hill (first straight 82 m, 146°; curve radius 90 m; take-off table 6.25 m, 168.5°). Equation 1 describes

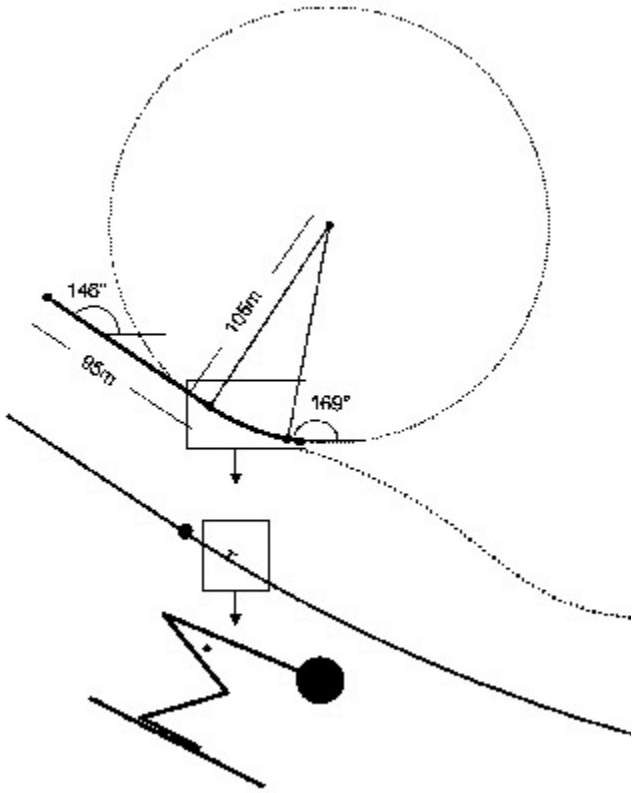

Figure 1 — Overview of in-run (solid line) and hill (dotted line) used in the simulation study (Granåsen K120, Trondheim). Boxed area is enlarged in the middle diagram. The jumper is again enlarged in the bottom diagram, where the dot indicates CoM.

the constraints of the curvature with regard to $\ddot{x}$ and $\ddot{y}$, the horizontal and vertical acceleration of the toe, and $\ddot{\varphi}_1$, the angular acceleration of the foot segment. The derivation of the equations and derivatives of s (hill slope) are given in the Appendix.

$$F_x - \tan\big(\arctan(s) + \arctan(c_f)\big)\, F_y = 0 \tag{1a}$$

$$\ddot{y} - s\ddot{x} = \frac{d^2y}{dx^2}\,\dot{x}^2 \tag{1b}$$

$$\ddot{\varphi}_1 - \frac{d\varphi_1}{ds}\frac{d^2y}{dx^2}\,\ddot{x} = \left\{ \frac{d^2\varphi_1}{ds^2}\left(\frac{d^2y}{dx^2}\right)^2 + \frac{d\varphi_1}{ds}\frac{d^3y}{dx^3} \right\}\dot{x}^2 \tag{1c}$$

where $\frac{dy}{dx} = s$, and $\varphi_1 = \arctan(s)$

For the straights, with infinite radius and constant slope, Equations 1b and 1c are simplified to:

$$\ddot{y} - s\ddot{x} = 0 \tag{2a}$$

$$\ddot{\varphi}_1 = 0 \tag{2b}$$

The transition from straight to curve is the transition from Equation 2a–b to 1b–c.

Effects of air resistance were modeled per segment and comprised two components, drag and lift (e.g., Virmavirta et al., 2001a). Lift force was estimated as being 10% of drag force. Drag force was dependent on the surface area perpendicular to movement direction, and therefore depended on the orientation of the individual segments. Surface area was approximated by length and width of each segment. For the upper body segment, depth was also estimated. When the upper body was directed perfectly parallel to the movement direction, the shoulders and head (helmet) created a surface into the airstream. Drag was calculated according to

$$F_d = c_d \, x \, 0.5 \, x \, \rho \, x \, A \, x \, v^2$$

where A is the surface area perpendicular to the direction of velocity v, ρ is air density, and c_d is drag coefficient, the latter being set either at 0.93 or at 0.31 (see below; Ettema & Bråten, 2004; Lien & Sætran, 2003; Virmavirta et al., 2001a). Each drag force was assumed to apply at the center of mass of each individual segment, thus not creating any external moment, and preventing the equations of motion from becoming unnecessarily complex. Total drag force was calculated by summing the four segmental drag forces; obviously, total drag force did not necessarily apply at the center of mass (CoM) of the entire body. Friction between ski and hill was calculated according to

$$F_f = c_f \, x \, F_{N,}$$

with c_f being the coefficient of friction and F_N being the normal force. Both drag and friction forces may contribute to the rotation of the entire body (see Figure 1). In the first instance we used relatively high values for c_d (0.93) and c_f (0.08) to create a relative large effect of resistance on rotation so that the principle was elucidated (high resistance simulation: HRS). A comparison was made with the lower values for c_d (0.31) and c_f (0.03) (low resistance simulation, LRS) afterward so that possible impact of these external factors could be evaluated. The values for c_d and c_f are considered to be the two extremes of a realistic range.

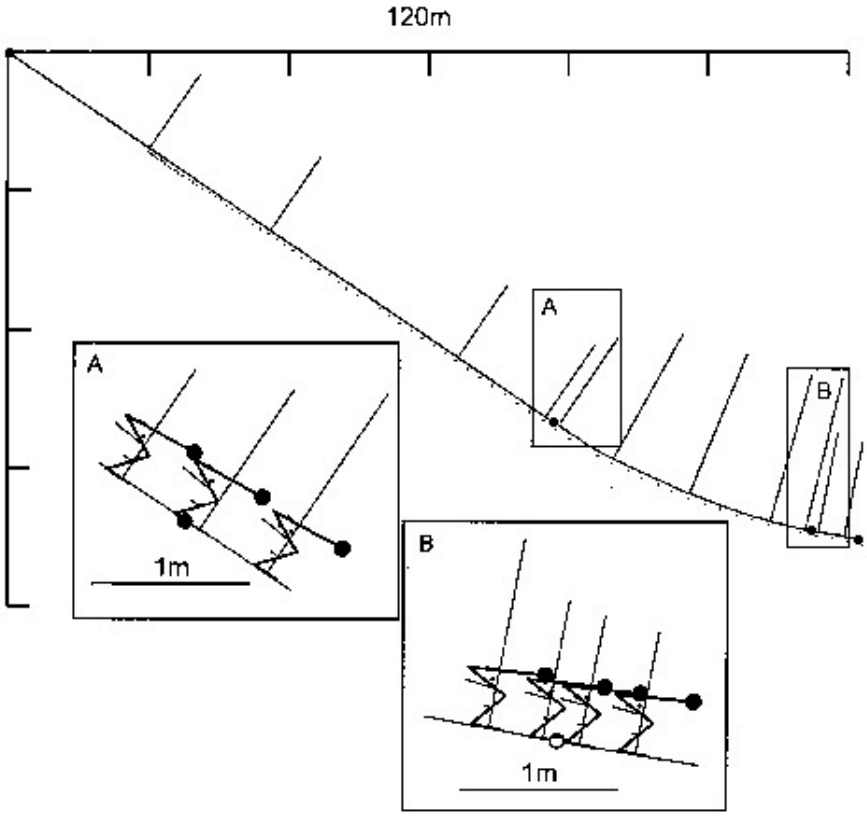

Figure 2 — Simulation of the in-run. Critical points of the in-run are indicated (circles). In the main diagram, each dot under the in-run indicates 0.1 s in time; the normal force is indicated at different times. Insets A and B show stick diagrams of the model at the critical moments (shifts of CoP) during the transitions into and out of the curve. The jumper continuously maintains body position by adjustment of joint torques. CoM is indicated by a dot; also indicated are normal force, drag per segment and total drag (thick line just below CoM), and snow friction.

Results

To make the rigid-dummy model reproduce take-off speeds obtained in practice (approx. 24.2 ms^{-1}, 87 kmh^{-1}), we released the model from a particular distance away from the curve entrance. With the settings for air resistance and friction used in this study, the model had to depart at 70-m distance from the curve entrance, i.e., 25 m below the top of the hill. A general impression of the dynamics is given in Figure 2. The main figure shows the normal forces. The dots just below the in-run indicate time ($\Delta t = 0.1$ s each dot). Note that the total time for the in-run (7.64 s) is relatively long compared to practice (5–6 s), which is mainly due to the relatively high resistance of drag and friction. Drag increases with the square of speed. The total air resistance creates a forward moment as the center of air resistance is somewhat

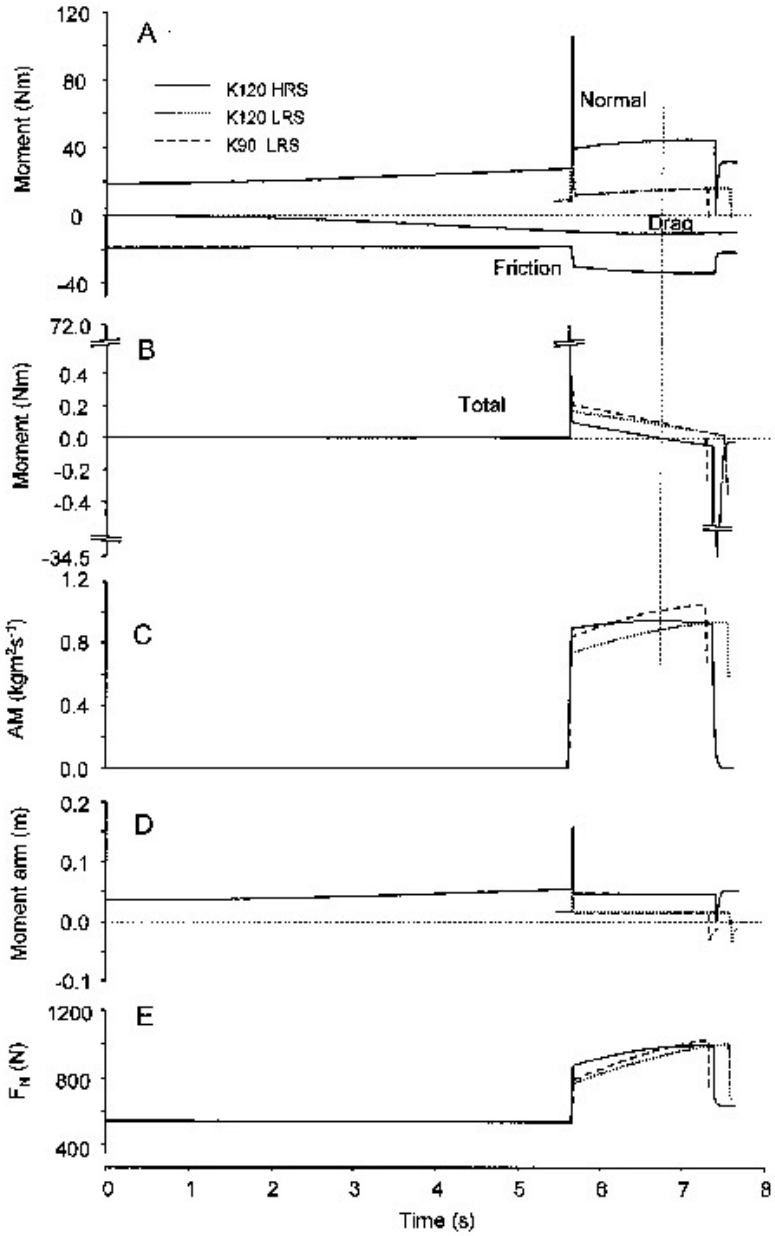

Figure 3 — Time traces of dynamic variables during the in-run. (A) Moments around the CoM of normal force, drag, and snow friction. For the low resistance conditions only the moment of F_N (not drag and friction) is shown. (B) Total external moment, i.e., sum of normal, drag, and snow friction moment. (C) Total angular momentum (AM) of the model. (D) Moment arm of normal force at CoM, the product of which is shown in Diagram A. (E) Normal force.

below the CoM. The line of action of the normal force (i.e., normal component of ground reaction force, not friction) continuously passes anteriorly to the CoM (i.e., the center of pressure, CoP, is located in front of the CoM) and is counteracting the moment created by drag.

Figure 3 shows several time traces of the in-run. At the curve entrance the model is kinematically forced to follow the curve, and the corresponding acceleration of CoM is reflected in a dramatic increase in normal force from 515 N to 970 N (0.88 G to 1.65 G) at the end of the curve (Figure 3E). Furthermore, the model is forced to initiate rotation, which is reflected in the backward moment (Figure 3B). The angular acceleration of the system as a whole is reflected in a brief and sudden shift of the CoP to the front (tip) of the foot (Figure 3D). Directly after the transition, the increased normal force passes closer to the CoM than during the first straight of the in-run (Figures 2A and 3D). This is the result of the interacting effects of increased F_N, the increased friction force, and the requirement of following the curvature of the in-run. The friction between in-run and skis increases at the entrance of the curve as the normal force increases dramatically. At the exit of the curve, more or less the opposite occurs. A sudden reduction of the normal force coincides with a rapid backward displacement of the CoP underneath the foot, so that it ends up passing through or just behind the CoM.

The situation is slightly different for the condition with less friction and drag (Figure 3, dotted curves). Because of lower resistance in the LRS, the model keeps increasing its speed to the end of the in-run, reaching 24.3 ms^{-1}. Departing at 47 m (compared to 70 m in high-resistance simulation, HRS, to obtain similar speed) before the curve, the total in-run time amounted to 5.85 s (7.64 s in HRS) and maximum drag was equal to 46.5 N (175 N in HRS). Overall, the simulation results seem to match empirical data from our wind tunnel experiments (Ettema & Bråten, 2004) and practice reasonably well. The normal force is comparable in both runs, but with reduced drag and friction it keeps increasing through the curve, and so does angular momentum. The moment of F_N is considerably reduced—the moment arm is smaller—and compensates less torque by drag and friction. The total moment (Figure 3B) remains positive (backward) throughout the curve but further follows a similar pattern as in the high-resistance simulation.

To study how the characteristics of the in-run affect the dynamics, we compared the K120 with the K90 for low friction conditions (Figure 3, dotted vs. dashed traces). The departure position in the K90 was chosen such that the peak velocity was about 1.11 ms^{-1} (4 kmh^{-1}) less than in the K120, as such a difference usually occurs in practice. The simulation results show that the angular momentum in the K90 hill exceeds that in the K120 by 10%, but normal forces differ only by 2% and the moment and moment arm of F_N differ even less.

The net joint moments that occur in the model during the transitions into and out of the curve are shown in Figure 4 for the K120 in-run under heavy resistance conditions. In the curve, increased joint moments were found that correspond with increased F_N and the small shift of CoP under the foot. It appeared that at curve entrance, considerable moment transients occurred over 10 ms in all three modeled joints. The maximal changes were approximately 100 Nm (ankle). The duration of the entire transient period, from the time that the front of the support base entered the curve to the time that the back of the base did so, was about 40 ms. All joint moments after the entrance of the curve were higher than during the straight. During the exit, rapid transients occurred in the ankle and hip (Figures 4D and 4F).

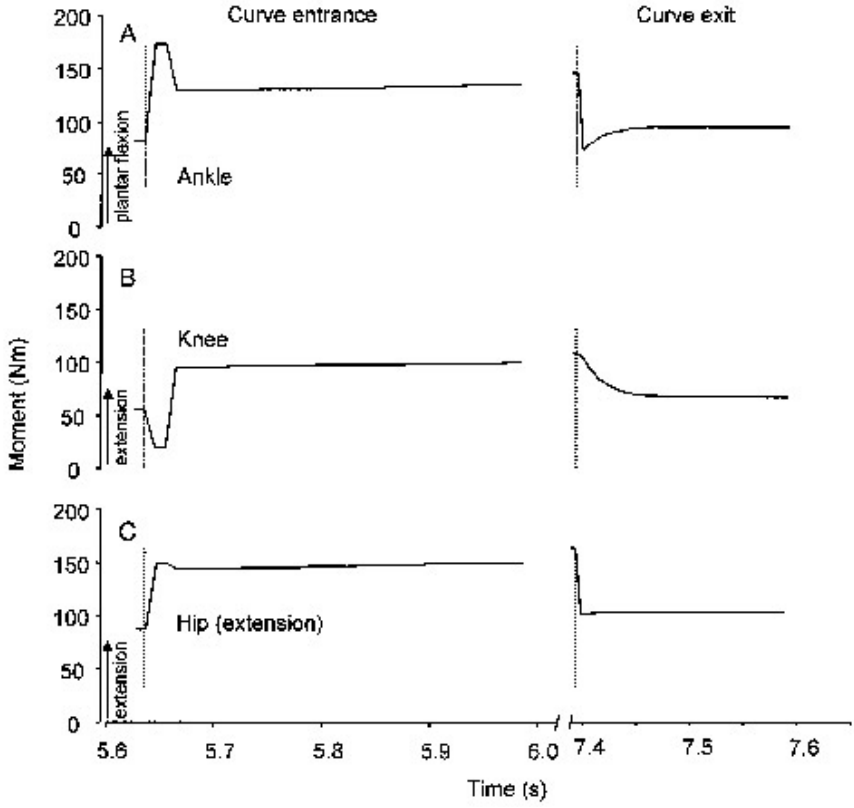

Figure 4 — Joint moments during and just after the entrance and exit of the curve for the K120 in-run under heavy resistance. The time points of entrance and exit are indicated by dotted vertical lines.

Discussion

The purpose of this study was to analyze the mechanical demands posed on an athlete when passing through the in-run of ski jumping in a static body position. We did this by simulating a rigid dummy, resembling the anthropometry of a ski-jumper, gliding down a K120 in-run and a K90 run under different conditions for snow friction and drag.

During the first straight, a slow increase of the backward moment of F_N occurs as a reaction on the increasing forward moment of air resistance, while the magnitude of F_N remains almost constant (a small reduction occurs because of the lift effect by air resistance). In real ski jumping, assuming the athlete wants to maintain a perfect static position, this can be achieved by subtle modifications in muscle activity generating small changes in hip, knee, and ankle moments. In combination with the external force at hand, these changes lead to an anterior shift of the CoP.

At the entrance of the curve, a quick increase in external moment occurs at the initiation of rotation (following the path of the hill demands a rapid increase of

angular momentum) after which the moment remains higher than in the straight. The increase in external moment in the curve is reflected in an increase of F_N rather than a shift of the CoP (i.e., change in moment arm; Figures 3A and 3D). The order of events is as follows: To follow a curvature of the in-run, the CoM needs to be accelerated; its velocity changes direction, which is reflected in the strongly increased F_N. This increase causes an enhanced snow friction force and thus an enhanced forward-moment-by-snow friction. The combination of this increased moment, the required angular momentum to follow the curve, and moment by drag determines the moment by F_N and thus the F_N moment arm. The exact size of the moment of F_N and therefore the location of CoP relative to CoM depends on the circumstances (e.g., drag and friction). Note that the increase of F_N by itself is a reflection of the curvilinear movement of the toes and therewith the CoM following the radius, and is not the cause of the body's angular acceleration with respect to the fixed coordinate system.

In reality, any flexibility of the skis would likely attenuate the high transient peaks in the traces of the moment of F_N. Even if an athlete were able to keep his or her body rigid, the flexible skis would make the changeover from the straight to curvature less abrupt. Given the average speed and length of the skis, the changeover would occur within 70 ms, about twice the duration of the peaks in the current simulations. This means that in reality the maximal attenuation of the transient peak would be about twofold, coinciding with a twofold increase of the duration, since the change in angular momentum does not depend on the flexibility of the skis. The exact attenuation depends on ski properties.

While the general principles of these events are similar for all conditions examined in this study, details depend on a combination of factors. Two important factors are drag and friction. With the center of drag being below the CoM, both drag and surface friction create a forward moment. Thus an increase of friction and drag tends to move the CoP in an anterior direction to the front of the foot.

The striking similarity in CoP position underneath the foot in the K90 and K120 (Figure 3) may be coincidental as it is only valid for the velocities obtained in this study. Still, these velocities were chosen similar to velocities achieved in reality. In any case the similar CoP positions indicate that an athlete would generate similar muscle moments in these conditions, supporting the findings of Virmavirta et al. (2001b) on push-off coordination. They found hardly any effect of hill size on muscle activation patterns. The fundamental issue here is the combination of centripetal force and change in angular momentum that is generated to go through the curve in static position. Both depend, albeit in different ways, on the athlete's velocity and on the radius of the curve of the hill.

The analysis thus far provides insight into the demands posed upon the athlete, not into how the athlete handles these demands. In the rigid-dummy model, (changes in) external forces, point of application (i.e., CoP), and moments occur purely as a reaction on the external constraints. In real ski jumping these changes are brought about by acting, presumably in an anticipatory manner, on the demands posed by the in-run characteristics. The changes in joint moments that occur reactively in the rigid dummy require from the athlete appropriate changes in muscle forces to be brought about by changes in muscle activation. During the straight, the normal force is less than gravity (0.88 G) because the athlete moves on a slope. Thus, less muscle moment is required to maintain the body position compared to moving level.

Toward the end of the curve, the normal force increases by a factor of 1.8

to about 1.65 G, the exact value depending on slope, speed, and radius. This is reflected by similar increases in joint moments (Figure 4). However, the knee moment increases by a larger factor, 1.96, as the CoP moves backward creating a larger moment arm for F_N at the knee. Still, even though they are substantial, the required joint moments lie well within the capabilities of an athlete (e.g., Aagaard, Simonsen, Andersen, Magnusson, & Dyhre-Poulsen, 2002; Bobbert & van Ingen Schenau, 1990; Ricard, Ugrinowitsch, Parcell, et al., 2005). However, the rate at which the moments need to change, particularly at the entrance and exit of the curve, may well be beyond an athlete's capability, even considering the effect of flexible skis. For example, Aagaard et al. (2002) examined the rate of force development in young males after a 14-week progressive heavy-resistance training program. They found a maximal rate of moment development of 2,000 Nms^{-1} during a maximal voluntary unilateral isometric knee extension. Ignoring possible bilateral deficit, this equals 80 Nm in 20 ms for a two-legged exercise. This is less than the findings from the rigid-dummy model, about 80 Nm within 10 ms in knee extension (Figure 4B).

The rate of force development levels for plantar flexion reported by Ricard et al. (2005) for female sprinters (600 Nms^{-1}) suggest that the requirements at the ankle are far beyond what is feasible. The perturbation of the curve entrance likely causes quick stretches in the musculature of an athlete, facilitating the required rapid force enhancement by mechanical and neural means. We performed preliminary simulations with a model incorporating skeletal-muscle tendon systems according to van Soest et al. (1993), in which muscle activation was kept constant. The results indicated that although the mechanical response of the muscle-tendon systems indeed helps generate the rapid moment increases, it is not sufficient to maintain position over a period beyond 200 ms: the model not only collapsed under the increased normal force but also generated too little angular momentum to follow the curve. Still, practice shows us that an athlete can perform this task with little difficulty, albeit not necessarily in a fully static position.

The remaining question, therefore, is what an athlete actually does with regard to muscle coordination in anticipation of the demands posed by the in-run dynamics. Obviously it is not easy to formulate optimization criteria, as the only apparent candidate, that of maintaining a perfectly still aerodynamic performance, is not likely realistic. Anecdotal evidence obtained from discussions with trainers and athletes suggests that an athlete attempts to maintain a "dynamic balance," which may be interpreted as a combination of minimizing movements and minimizing changes of CoP under the foot. This last factor is deemed crucial for a good push-off action. It is clear that experimental data, specifically measurements of ground reaction forces, are required to elucidate this issue further.

The exit of the curve is of special interest as it coincides with the start of the actual push-off action. Without attempting to discuss the muscle coordination pattern required for a successful take-off, the following can be said. At the end of the curve the jumper has a nearly constant but high positive angular momentum (i.e., backward). This momentum needs to be removed, and for a good take-off probably needs to change into a slightly negative value (forward) at the end of take-off. The most striking finding during this transition is the rapid shift of the line of action of the normal force from just in front of CoM to far behind (toward the heel). This rapid transition occurs because of the kinematic forcing (stopping backward rotation). An athlete does not need to make the same performance as he or she has already started

push-off, or is about to. But once again, the moment transients for a rigid dummy are illustrative for the highly specific conditions and requirements that are imposed in ski jumping, in this case at about the time the push-off is initiated.

It should be noted here that if an athlete is to lose the backward momentum, it is not enough to merely be exiting the curve as in the case for a rigid dummy. The athlete needs to alter muscle forces to stop the rotation of all body segments. More insight into the impact of these requirements on the push-off action can be obtained by implementing muscle-tendon units in the current model and performing optimization exercises of the push-off action. Comparisons with simulations of different dryland-training exercises may prove useful for training praxis.

References

Aagaard, P., Simonsen, E.B., Andersen, J.L., Magnusson, P., & Dyhre-Poulsen, P. (2002). Increased rate of force development and neural drive of human skeletal muscle following resistance training. *Journal of Applied Physiology*, **93**, 1318-1326.

Bobbert, M.F., Houdijk, H., de Koning, J.J., & de Groot, G. (2002). From a one-legged vertical jump to the speed-skating push-off: A simulation study. *Journal of Applied Biomechanics*, **18**, 28-45.

Bobbert, M.F., & van Ingen Schenau, G.J. (1990). Isokinetic plantar flexion: Experimental results and model calculations. *Journal of Biomechanics*, **23**, 105-119.

Ettema, G.J.C., & Bråten, S. (2004). Effect of air resistance on balanced position in the in-run. Unpublished report for Olympiatoppen as part of the project "*Influence of Body Posture on Performance in Cross-Country Skiing and Ski-Jump – 2003*."

Komi, P.V., & Virmavirta, M. (2000). Determinants of successful ski-jumping performance. In V. Zatsiorski (Ed.) *Biomechanics in sport – Performance enhancement and injury prevention, Olympic encyclopaedia of sports medicine, Vol. IX* (pp. 349-362). Oxford: Blackwell Scientific.

Lien, T.E., & Sætran, L. (2003). Fysiske krefter på skihopper [Physical forces on a ski jumper]. Unpublished report for Olympiatoppen as part of the project "*Influence of Body Posture on Performance in Cross-Country Skiing and Ski-Jump – 2003*."

Pandy, M.G., Zajac, F.E., Sim, E., & Levine, W.S. (1990). An optimal control model for maximum-height human jumping. *Journal of Biomechanics*, **23**, 1185-1198.

Ricard, M.D., Ugrinowitsch C., Parcell A.C., Hilton S., Rubley M.D., Sawyer R., & Poole C.R. (2005). Effects of rate of force development on EMG amplitude and frequency. *International Journal of Sports Medicine*, **26**, 66-70.

Tveit, P., & Pedersen, P. (1981). Forces in the take-off in ski-jumping. In A. Morecki, K. Fidlus, K. Kedzior, & A. Wit (Eds.), *Biomechanics VII-B* (pp. 472-477), Baltimore: University Park Press.

van Soest, A.J., Schwab, A.L., Bobbert, M.F., & van Ingen Schenau, G.J. (1993). The influence of biarticularity of the gastrocnemius muscle on vertical-jumping achievement. *Journal of Biomechanics*, **26**, 1-8.

Virmavirta, M., Kikeväs, J., & Komi, P.V. (2001a). Take-off aerodynamics in ski jumping. *Journal of Biomechanics*, **34**, 465-470.

Virmavirta, M., & Komi, P.V. (1989). The takeoff force in ski jumping. *International Journal of Sport Biomechanics*, **5**, 248-257.

Virmavirta, M., & Komi, P.V. (1993). Measurement of take-off forces in ski jumping. Parts I & II. *Scandinavian Journal of Medicine and Science in Sports*, **3**, 229-243.

Virmavirta, M., Perttunen, J., & Komi, P.V. (2001b). EMG activities and plantar pressures during ski jumping take-off on three different sized hills. *Journal of Electromyography and Kinesiology*, **11**, 141-147.

Appendix

The description in x and y coordinates of the hill and its derivatives are given in Equations A1–A4 for the curvature (circle with radius *r*). The x and y offsets are omitted in Equation A1 for simplicity.

$$y = -\sqrt{r^2 - x^2} \tag{A1}$$

$$\frac{dy}{dx} = \frac{1}{\sqrt{r^2 - x^2}} x = s \tag{A2}$$

$$\frac{d^2y}{dx^2} = \frac{r^2}{\left(r^2 - x^2\right)\sqrt{r^2 - x^2}} = s2 \tag{A3}$$

$$\frac{d^3y}{dx^3} = \frac{6x}{\left(r^2 - x^2\right)^2 \sqrt{r^2 - x^2}} = s3 \tag{A4}$$

For the straights, these equations regress to

$$y = s_i x \tag{A5}$$

$$\frac{dy}{dx} = s_i \tag{A6}$$

$$\frac{d^2y}{dx^2} = 0 \tag{A7}$$

$$\frac{d^3y}{dx^3} = 0 \tag{A8}$$

where $s_i = \tan(\varphi_i)$, i = first straight, takeoff table. The general chain rule for second derivatives:

$$\frac{d^2y}{dt^2} = \frac{d^2y}{dx^2}\left(\frac{dx}{dt}\right)^2 + \frac{dy}{dx}\frac{d^2x}{dt^2} \tag{A9}$$

is transformed to Equation 1b:

$$\frac{d^2y}{dt^2} - \frac{dy}{dx}\frac{d^2x}{dt^2} = \frac{d^2y}{dx^2}\left(\frac{dx}{dt}\right)^2 \rightarrow$$

$$\ddot{y} - s\ddot{x} = \frac{d^2y}{dx^2}\dot{x}^2 \tag{1b}$$

$$\ddot{y} - s\ddot{x} = s2\dot{x}^2 = \frac{r^2}{\left(r^2 - x^2\right)\sqrt{r^2 - x^2}}\dot{x}^2 \tag{A10}$$

Equation A10 is found by substituting Equation A2 into 1b.

The description for φ_1 in Equation 1c is found as follows:

$$\frac{ds}{dt} = \frac{ds}{dx}\frac{dx}{dt} = \frac{d^2y}{dx^2}\frac{dx}{dt} = s2\frac{dx}{dt}$$

$$\frac{d^2s}{dt^2} = \frac{d^3y}{dx^3}\left(\frac{dx}{dt}\right)^2 + \frac{d^2y}{dx^2}\frac{d^2x}{dt^2} = s3\left(\frac{dx}{dt}\right)^2 + s2\frac{d^2x}{dt^2}$$

$$\varphi_1 = \arctan(s)$$

$$\frac{d\varphi_1}{ds} = \frac{1}{1+s^2} = h1$$

$$\frac{d^2\varphi_1}{ds^2} = \frac{-2}{\left(1+s^2\right)^2}s = h2$$

$$\frac{d^2\varphi_1}{dt^2} = \frac{d^2\varphi_1}{ds^2}\left(\frac{ds}{dt}\right)^2 - \frac{d\varphi_1}{ds}\frac{d^2s}{dt^2} = h2\left(\frac{ds}{dt}\right)^2 + h1\frac{d^2s}{dt^2} = \ldots$$

$$\ldots h2\left(s2\frac{dx}{dt}\right)^2 + h1\left\{s3\left(\frac{dx}{dt}\right)^2 + s2\frac{d^2x}{dt^2}\right\} \tag{A11}$$

Equation A11 can be rewritten as

$$\ddot{\varphi}_1 - h1\,s2\,\ddot{x} = \left(h2\,s2^2 + h1\,s3\right)\dot{x}^2$$

or

$$\ddot{\varphi}_1 - \frac{d\varphi_1}{ds}\frac{d^2y}{dx^2}\ddot{x} = \left\{\frac{d^2\varphi_1}{ds^2}\left(\frac{d^2y}{dx^2}\right)^2 + \frac{d\varphi_1}{ds}\frac{d^3y}{dx^3}\right\}\dot{x}^2 \tag{1c}$$